

AB– and BA–GMRES Methods for X-Ray CT with an Unmatched Back Projector

Per Christian Hansen

Technical University of Denmark

Joint work with

Ken Hayami, NII, Tokyo

Keiichi Morikuni, Univ. Tsukuba

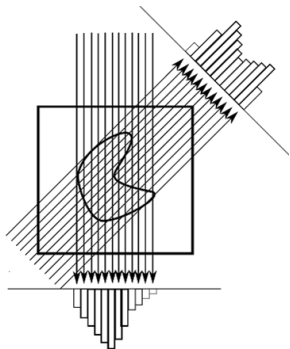
Emil Sidky, Univ. Chicago



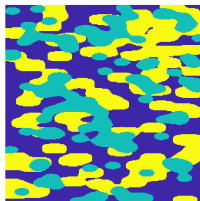
Prologue: X-Ray CT in 2D – and the Radon Transform

The Principle

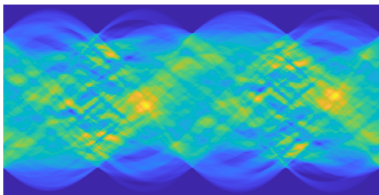
Send X-rays through the object f at many angles, and measure the attenuation g .



$f = 2\text{D object/image}$



$g = \mathcal{R}f = \text{Radon transform of } f$
 $= \text{sinogram}$



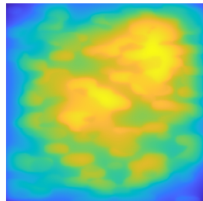
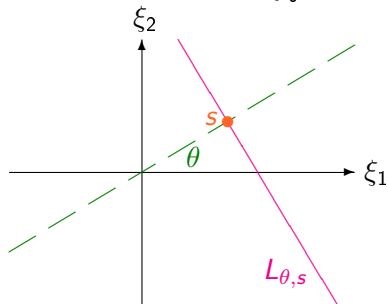
Prologue: Forward and Back Projections

Forward projection \mathcal{R} , the Radon transform models the scanner physics via integration of the function f along lines $L_{\theta,s}$

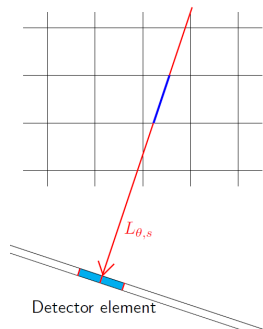
$$\mathcal{R}[f](\theta, s) = \int_{L_{\theta,s}} f(\xi_1, \xi_2) d\ell = g(\theta, s) = \text{sinogram} .$$

Back projection $\mathcal{B} = \text{adjoint}(\mathcal{R})$, an abstraction, smears g back along $L_{\theta,s}$

$$\mathcal{B}[g](\xi_1, \xi_2) = \int_0^{2\pi} g(\theta, \xi_1 \cos \theta + \xi_2 \sin \theta) d\theta .$$

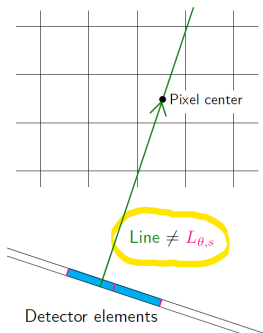


Ray/Pixel Driven Discretization Models



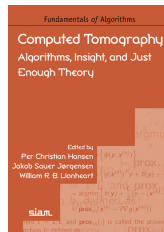
Forward line model

Ray driven



Back projection model

Pixel driven



Details here

Forward line model: start from detector element centers.

Back projection model: start from image pixel centers and interpolate detector element values.

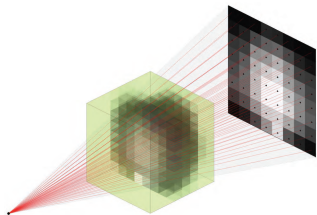
Projectors and Matrices

Multiplication with $A \iff$ action of **forward projector** \mathcal{R} .

Multiplication with $B \iff$ action of **back projector** $B = \text{adjoint}(\mathcal{R})$.

When we can store A (it is *sparse*), then we can use $B = A^T$, and solve the normal equations $A^T A x = A^T b$ associated with the least squares problem, with $x = \text{vec}(\text{image})$ and $b = \text{vec}(\text{sinogram})$.

But storage can be problematic. 3D example: 1000 projection angles, 1000×1000 detector elements, $1000 \times 1000 \times 1000$ voxels \rightarrow number of non-zeros in A is of the order $10^{12} \sim$ several Terabytes of memory.



When A is *too large to store*, we must use **matrix-free multiplications** of the **forward projector** and the **back projector** – cf. the discr. models.

Ray and pixel driven models $\rightarrow B \neq A^T \rightarrow$ unmatched projector pair.

Solve the Unmatched Normal Equations

Classical iterative methods (e.g., Cimmino, SIRT, CGLS) require $B = A^T$.
Alternatively, we can solve the **unmatched normal equations**

$$\text{UNE: } \boxed{BAx = Bb} \quad \text{or} \quad \boxed{AB y = b, \quad x = B y}$$

We will use **GMRES** (Saad, Schultz, 1986), a very efficient iterative method for solving systems

$$\boxed{Mx = d} \quad \text{with a square and nonsymmetric matrix } M.$$

We skip the implementation details here, and just remind that in the k th step, the iterate x^k of GMRES solves the problem

$$\min_x \|Mx - d\|_2 \quad \text{subject to} \quad x \in \mathcal{K}_k(M, d),$$

with the *Krylov subspace*

$$\mathcal{K}_k(M, d) = \text{span}\{d, Md, M^2d, \dots, M^{k-1}d\}.$$

AB-GMRES and BA-GMRES

We can formulate *specialized versions* of GMRES for the UNEs:

BA-GMRES solves $BAx = Bb$.

AB-GMRES solves $AB y = b, x = B y$.

Both methods use the same Krylov subspace $\mathcal{K}_k(BA, Bb)$ for the solution, but they use different objective functions.

Advantages:

- both methods always converge,
- no need for relaxation parameter,
- fairly simple to implement → next page.

▷ K. Hayami, J.-F. Yin, T. Ito, *GMRES methods for least squares problems*, SIAM J. Matrix Anal. Appl., 31 (2010), 2400–2430.

▷ H. K. Hayami, K. Morikuni, *GMRES methods for tomographic reconstruction with an unmatched back projector*, J. Comp. Appl. Math., 413 (2022), 114352.

The ABBA Algorithms

Algorithm AB-GMRES

Choose initial x_0
 $r_0 = b - Ax_0$
 $w_1 = r_0 / \|r_0\|_2$
for $k = 1, 2, \dots$
 $q_k = AB w_k$
 for $i = 1, 2, \dots, k$
 $h_{i,k} = q_k^\top w_i$
 $q_k = q_k - h_{i,k} w_i$
 endfor
 $h_{k+1,k} = \|q_k\|_2$
 $w_{k+1} = q_k / h_{k+1,k}$
 $y_k = \arg \min_y \| \|r_0\|_2 e_1 - H_k y \|_2$
 $x_k = x_0 + B [w_1, w_2, \dots, w_k] y_k$
 $r_k = b - Ax_k$
 stopping rule goes here
endfor

Algorithm BA-GMRES

Choose initial x_0
 $r_0 = Bb - BAx_0$
 $w_1 = r_0 / \|r_0\|_2$
for $k = 1, 2, \dots$
 $q_k = BA w_k$
 for $i = 1, 2, \dots, k$
 $h_{i,k} = q_k^\top w_i$
 $q_k = q_k - h_{i,k} w_i$
 endfor
 $h_{k+1,k} = \|q_k\|_2$
 $w_{k+1} = q_k / h_{k+1,k}$
 $y_k = \arg \min_y \| \|r_0\|_2 e_1 - H_k y \|_2$
 $x_k = x_0 + [w_1, w_2, \dots, w_k] y_k$
 $r_k = b - Ax_k$
 stopping rule goes here
endfor

MATLAB and Python software available from PCH at

<https://people.compute.dtu.dk/pcha/ABBA>

and in TIGRE: Tomographic Iterative GPU-based Reconstruction Toolbox

<https://github.com/CERN/TIGRE>

Obligatory Slide with Many Equations

Hayami, Yin, Ito (2010), H, Hayami, Morikuni (2022)

AB-GMRES solves $\min_y \|AB y - b\|_2$, $x = B y$

- ▷ $\min_x \|A x - b\|_2 = \min_y \|AB y - b\|_2$ holds for all b if and only if $\text{range}(AB) = \text{range}(A)$, e.g., if $\text{range}(B) = \text{range}(A^T)$.
- ▷ Monotonic decay of $\|A x^k - b\|_2$.
- ▷ Equivalent to LSQR when $B = A^T$.

BA-GMRES solves $\min_x \|BA x - B b\|_2$

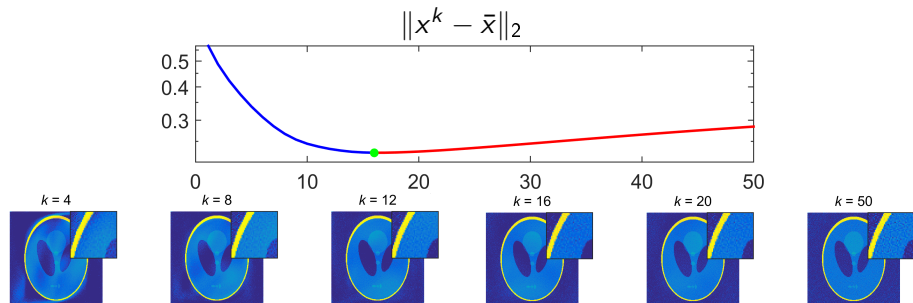
- ▷ the problems $\min_x \|A x - b\|_2$ and $\min_x \|BA x - B b\|_2$ are equivalent for all b if and only if $\text{range}(B^T BA) = \text{range}(A)$, e.g., if $\text{range}(B^T) = \text{range}(A)$.
- ▷ Monotonic decay of $\|BA x^k - B b\|_2$.
- ▷ Equivalent to LSMR when $B = A^T$.

Conditions are difficult/impossible to check in a given CT problem.

Iterative Methods: Noisy Data Gives Semi-Convergence

The right-hand side b (the data) is a sum of noise-free data $\bar{b} = A\bar{x}$ from the ground-truth image \bar{x} plus a noise component e :

$$b = A\bar{x} + e, \quad \bar{x} = \text{ground truth}, \quad e = \text{noise}.$$

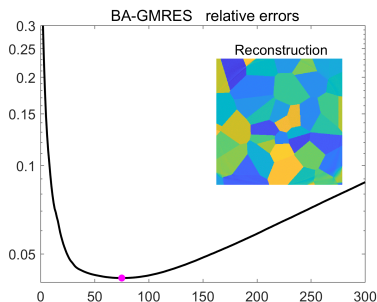
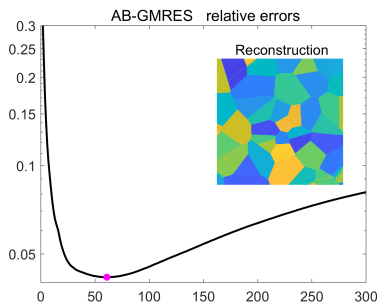


- In the **initial iterations** x^k approaches the unknown ground truth \bar{x} .
- During **later iterations** x^k converges to the undesired $x^{\text{naive}} = A^{-1}b$.
- **Stop the iterations** when the convergence behavior changes.

ABBA Reconstruction Errors $\|x^k - \bar{x}\|_2 / \|\bar{x}\|_2$

Image has 420×420 pixels, 600 projection angles, 420 detector pixels.

A and B generated with GPU-ASTRA software; A is $252\,000 \times 176\,400$.

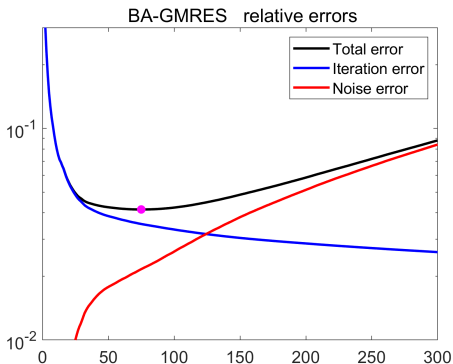


- **Semi-convergence** is evident for both methods.
- Same minimum reconstruction error $\|x^k - \bar{x}\|_2 / \|\bar{x}\|_2 \approx 0.042$ for both.
- Slightly fewer iterations for AB-GMRES in this example.
- Storage for Krylov bases – AB-GMRES: $m \times k$ – BA-GMRES: $n \times k$.

Error Propagation in BA-GMRES

Let \bar{x}^k denote the iterates for a noise-free right-hand side. We consider:

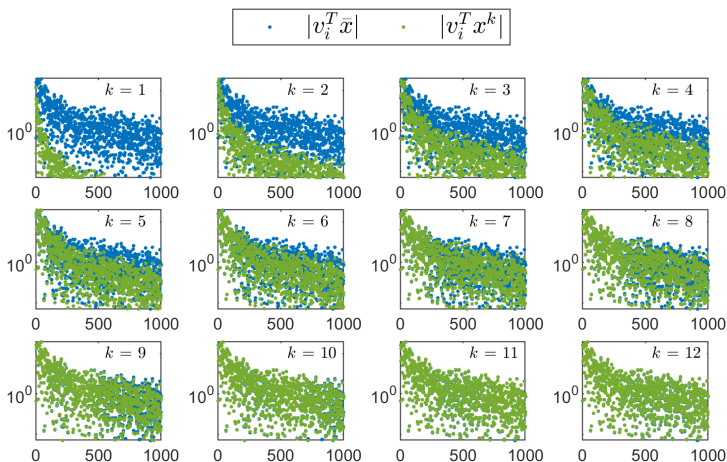
$$\underbrace{x^k - \bar{x}}_{\text{total error}} = \underbrace{x^k - \bar{x}^k}_{\text{noise error}} + \underbrace{\bar{x}^k - \bar{x}}_{\text{iteration error}}$$



Both errors are monotonic in this example – but no guarantee for this.

Semi-Convergence of BA-GMRES ★ SVD Insight

Recall: $b = A\bar{x} + e$, $\bar{x} = \text{ground truth}$, $\|e\|_2/\|\bar{b}\|_2 = 0.001$ Gaussian.



- As k increases we capture more and more SVD components in x^k .
- At $k = 11$ we already capture the first 1000 SVD components.

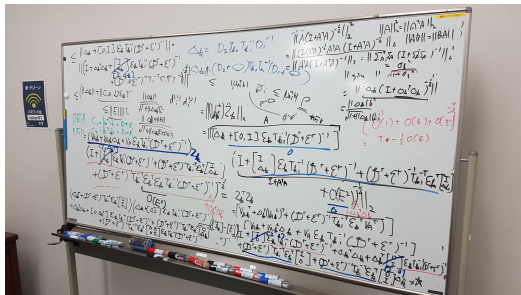
Semi-Convergence of BA-GMRES ★ Subspaces

In our numerical example, $\|B - A^T\|_F / \|B\|_F \approx 0.15$.

So how come we can still compute good reconstructions?

- Compare the Krylov subspace with the SVD subspace.

We are working on it ...



Stopping Rules

We must terminate the iterations at the point of **semi-convergence**.

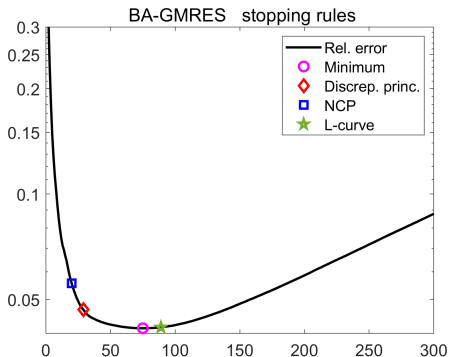
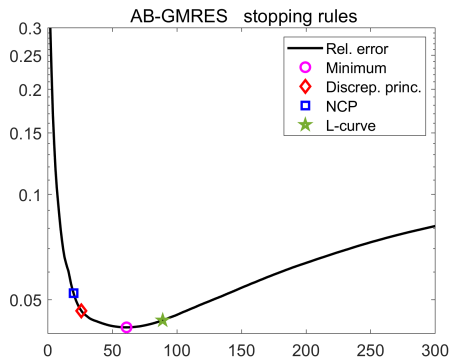
- **Discrepancy principle (DP)**: terminates the iterations as soon as the residual norm is smaller than the noise level:

$$k_{\text{DP}} = \text{the smallest } k \text{ for which } \|b - Ax^k\|_2 \leq \tau \|e\|_2$$

where $\tau \geq 1$ = safety factor when we have a rough estimate of $\|e\|_2$.

- **NCP criterion**: uses the Normalized Cumulative Periodogram to perform a spectral analysis of the residual vector $b - Ax^k$ and identifies when the residual is close to being white noise – which indicates that all available information has been extracted from the noisy data.
- **L-curve criterion**: locates the “corner” of the L-shaped point set $(\log \|b - Ax^k\|_2, \log \|x^k\|_2)$.

Stopping Rules in Action



Both the **discrepancy principle** and the **NCP criterion** stop too early.
The **L-curve criterion** stops too late.

A topic for further research, related to all iterative regularization methods.

Computational experiments with real data by:

Emil Y. Sidky, Department of Radiology, University of Chicago.

- Cone-beam CT data from an Epica Pegaso veterinary CT scanner.
- 180 projections taken uniformly over one circular rotation.
- Physical “quality assurance” (QA) phantom \longrightarrow
- Detector: 1088×896 pixels of size $(0.278\text{mm})^2$.
- 3D reconstruction: $1024 \times 1024 \times 300$ voxel grid.



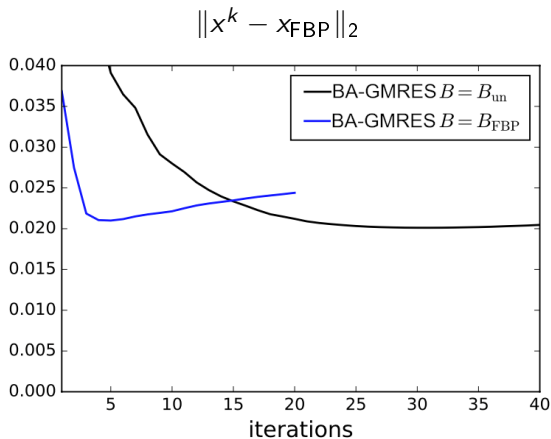
Ray-driven projector A . Two choices of B :

- B_{un} = voxel-driven back projection, linear interpolation on detector.
- $B_{\text{FBP}} = B_{\text{un}}F$ = filtered back-projection, where F = ramp filter.

“Reconstruction Error”

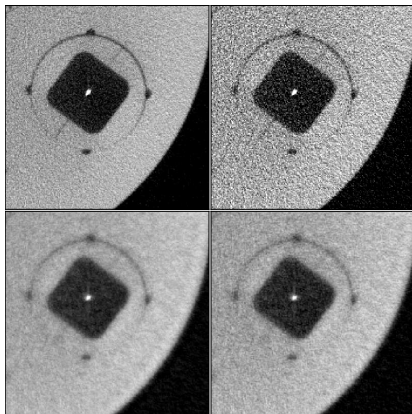
Real data from a physical phantom \Rightarrow no ground truth \bar{x} .

Instead we use a high-quality FBP reconstruction x_{FBP} .



With both B -matrices we observe semi-convergence.

Reconstruction, Mid-Slice Region of Interest



Top left: reference $x_{\text{FBP}} = \text{FBP}$ reconstructed image from 720 views.

Top right: FBP reconstructed images from 180 views.

Bottom left: BA-GMRES image, $B = B_{\text{un}}$, $k = 29$ iterations, 180 views.

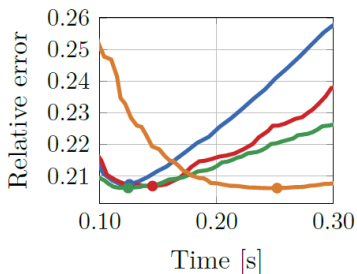
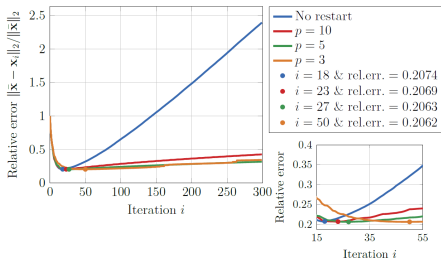
Bottom right: BA-GMRES image, $B = B_{\text{FBP}}$, $k = 4$ iterations, 180 views.

Epilogue: Restart of the ABBA Methods

Must compute and store the orthonormal basis for the Krylov subspace.
But orthonormalization is time consuming, and storage may be prohibitive.

Restart solves these problems; more iterations are necessary, but the computing time does not deteriorate.

Convergence of BA-GMRES for Fan Beam Geometry



M. Knudsen, *ABBA Iterative Methods for X-Ray Computed Tomography*,
MSc Thesis, DTU, 2023 [link](#)

Unmatched projector pairs★

- Need efficient iterative reconstruction methods for unmatched pairs.
- Modify a classical method, e.g., as in the Shifted BA Iteration.
- Use a method that solves the unmatched normal equations \rightarrow ABBA.

★New matched pair: *K. Bredies & R. Huber, Convergence analysis of pixel-driven Radon and fanbeam transforms, SIAM J. Numer. Anal., 59 (2021), 1399–1432.*

Convergence

- Good understanding of convergence for noise-free data.
- Emerging: understanding of **semi-convergence** for noisy data.

Future

- More theory about semi-convergence for GMRES.

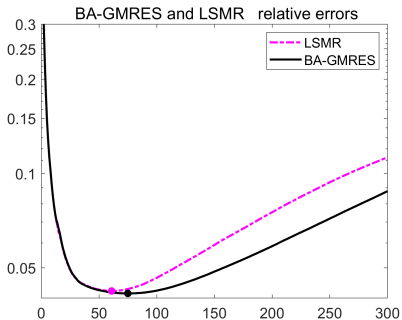
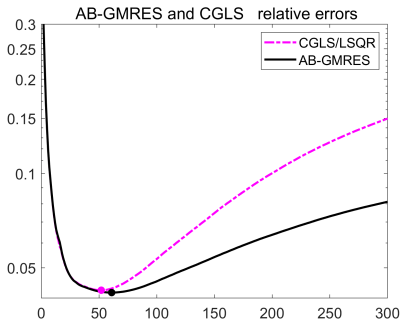
Semi-convergence of CGLS is well understood; but only few results have been obtained for GMRES.

- **Calvetti, Lewis, Reichel (2002)**: if the noise-free data lies in a finite-dimensional Krylov subspace, and if GMRES is equipped with a suitable stopping rule, then the GMRES-solution tends towards the exact solution \bar{x} as the noise goes to zero.
- **Gazzola, Novati (2016)**: if the discrete Picard condition (DPC) is satisfied and if the left singular vectors of the Hessenberg matrices of two consecutive GMRES steps resemble each other – then the Hessenberg systems in GMRES also satisfy the DPC.

The difficulty is that we cannot analyze GMRES by means of the SVD of A . A complete understanding has not emerged yet. Here we rely on some preliminary analysis and insight from numerical experiments.

Appendix: Comparison with CGLS/LSQR and LSMR

If $B = A^T$ then AB-GMRES = CGLS/LSQR and BA-GMRES = LSMR.



Recall: for large-scale problems we do not have a choice; we must use B .
The good news is that the reconstruction error does not deteriorate, compared with using A^T (in this example, the error is slightly smaller).